

Host-Derived Tumor Endothelial Marker 8 Promotes the Growth of Melanoma

Mike Cullen,¹ Steven Seaman,¹ Amit Chaudhary,¹ Mi Young Yang,¹ Mary Beth Hilton,^{1,2} Daniel Logsdon,² Diana C. Haines,³ Lino Tessarollo,⁴ and Brad St. Croix¹

¹Tumor Angiogenesis Section, Mouse Cancer Genetics Program, ²Basic Research Program, Science Applications International Corporation, ³Pathology/Histotechnology Laboratory, Science Applications International Corporation, and ⁴Mouse Cancer Genetics Program, National Cancer Institute-Frederick, Frederick, Maryland

Abstract

Tumor endothelial marker 8 (TEM8) was initially identified as a gene overexpressed in the vasculature of human tumors and was subsequently identified as an anthrax toxin receptor. To assess the functional role of TEM8, we disrupted the TEM8 gene in mice by targeted homologous recombination. TEM8^{-/-} mice were viable and reached adulthood without defects in physiologic angiogenesis. However, histopathologic analysis revealed an excess of extracellular matrix in several tissues, including the ovaries, uterus, skin, and periodontal ligament of the incisors, the latter resulting in dental dysplasia. When challenged with B16 melanoma, tumor growth was delayed in TEM8^{-/-} mice, whereas the growth of other tumors, such as Lewis lung carcinoma, was unaltered. These studies show that host-derived TEM8 promotes the growth of certain tumors and suggest that TEM8 antagonists may have utility in the development of new anticancer therapies. [Cancer Res 2009;69(15):6021–6]

Introduction

The vascularization of solid tumors provides tumor cells with an essential supply of oxygen and nutrients and is considered a prerequisite for the sustained growth and spread of cancer (1). The successful design of rational new agents that can inhibit tumor growth by destroying or preventing the growth of tumor blood vessels depends on an intimate molecular understanding of tumor angiogenesis. Global analyses of gene expression of endothelial cells lining the tumor blood vessels of human colorectal cancer have led to the identification of a series of genes called tumor endothelial markers (TEM; ref. 2). Of these, TEM8 is of particular interest because of its overexpression in tumor vessels of multiple tumor types, cell surface localization, high conservation among species, and lack of detectable expression in the angiogenic vessels of the corpus luteum (2–4). The predominant form of TEM8 is a single-pass transmembrane glycoprotein of approximately 80 to 85 kDa containing an extracellular von Willebrand type A domain and a large cytoplasmic tail. *In vitro* TEM8 has been found to bind collagen types I and VI (3, 5, 6). Both TEM8 and capillary

morphogenesis protein 2 (CMG2), its closest homologue, have been identified as anthrax toxin receptors and are therefore also known as ANTXR1 and ANTXR2, respectively (7, 8). Interestingly, anthrax lethal toxin, composed of lethal toxin and protective antigen, displayed potent antitumor activity in preclinical tumor models when judiciously administered to mice at nontoxic doses (9–13). Up-regulation of TEM8 in tumor vessels may help to explain the tumoricidal activity of anthrax lethal toxin *in vivo*, but CMG2, also expressed in endothelial cells, could potentially play a role. To better understand the normal functional role of TEM8, we disrupted the TEM8 gene in mice by homologous recombination. These studies show that TEM8 plays an important role in normal extracellular matrix (ECM) homeostasis and the growth of certain tumor types, such as melanoma.

Materials and Methods

See Supplementary Data for additional methods.

Generation of TEM8 knockout mice. The TEM8 knockout (KO) strategy is described in detail in Supplementary Data. TEM8 KO mice were originally made on a mixed 129SvJae/C57BL6 genetic background and have been backcrossed >10 generations onto a C57BL6 background. Each of the experiments described herein was performed on mice that had been backcrossed at least five generations and were at least 95% C57BL6.

Endothelial purification, reverse transcription-PCR, and quantitative real-time PCR. Purification of endothelial cells from tumors or normal tissues, mRNA isolation, cDNA synthesis, and reverse transcription-PCR (RT-PCR) or quantitative real-time PCR (qPCR) were performed as previously described (14) using rat anti-mouse CD31 antibodies (BD Pharmingen) for the endothelial cell isolation. Primers can be found in Supplementary Table S1.

Histologic examination. A comprehensive set of tissues from six TEM8^{+/+} and eight TEM8^{-/-} 6- to 8-mo-old mice was fixed in formalin, routinely processed, paraffin embedded, sectioned at 5 μ m, stained with H&E and trichrome, and evaluated by a boarded veterinary pathologist (D.C.H.). For immunofluorescence staining, see Supplementary Materials and Methods.

Results and Discussion

To disrupt the TEM8 gene in mice, a targeting vector was designed to remove the first exon of TEM8, which contains part of the TEM8 promoter, the start codon, and the signal peptide (Fig. 1A; Supplementary Materials and Methods). The introduction of lox-p sites into the genomic sequence upstream and downstream of exon 1 allowed the removal of this exon by crossing mice with a transgenic deleter strain that constitutively expresses cre recombinase (β -actin-Cre). Genotyping of 987 offspring from TEM8^{+/+} heterozygous intercrosses using a PCR assay (Fig. 1B, left) revealed TEM8^{-/-} mice at the expected Mendelian frequency (Supplementary Table S2). To determine if TEM8 KO mice were able to breed, we crossed TEM8^{-/-} males to TEM8^{+/+} females and

Note: Supplementary data for this article are available at Cancer Research Online (<http://cancerres.aacrjournals.org/>).

M. Cullen and S. Seaman contributed equally to this work.

The content of this publication does not necessarily reflect the views or policies of the DHSS, nor does mention of trade names, commercial products, or organizations imply endorsement by the U.S. Government.

Requests for reprints: Brad St. Croix, National Cancer Institute-Frederick, Building 560, P. O. Box B, Frederick, MD 21702-1201. Phone: 301-846-7456; Fax: 301-846-7017; E-mail: stcroix@ncifcrf.gov.

©2009 American Association for Cancer Research.

doi:10.1158/0008-5472.CAN-09-1086

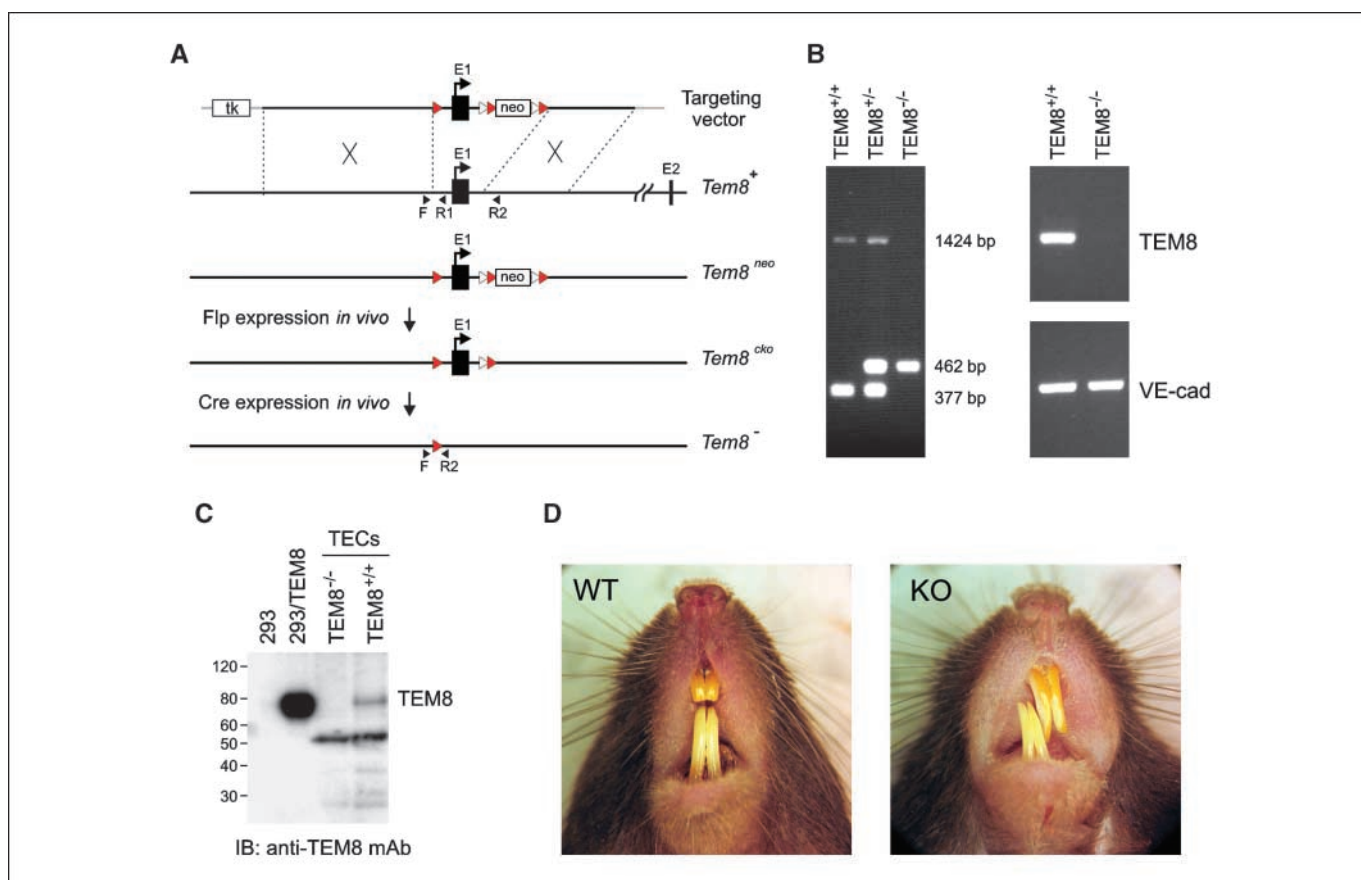


Figure 1. Targeting vector and evidence of TEM8 loss *in vivo*. *A*, a conditional *TEM8* targeting vector was generated by introducing lox-p sites (red arrowheads) into the genomic sequence upstream and downstream of exon 1. Following electroporation, embryonic stem cell clones with a floxed *TEM8*^{neo} allele were identified by Southern blotting (data not shown) and used to generate chimeric mice and achieve germ-line transmission of the *TEM8*^{neo} allele. *TEM8*^{+/neo} mice were crossed with a β -actin-Cre deleter strain to generate mice with a *TEM8*-null (*TEM8*⁻) allele. Frt sites (white arrowheads) were also introduced on either side of the neomycin cassette to allow its removal with Flp recombinase generating a conditional KO allele (*TEM8*^{cko}). Forward arrow, start codon and signal peptide; TK, thymidine kinase cassette used for negative selection; neo, neomycin cassette used for positive selection; black arrowheads, location of forward and reverse PCR primers used for genotyping. *B*, left, genotyping of genomic DNA by PCR; right, RT-PCR was used to detect mRNA expression. Note that *TEM8* expression is only detectable in *TEM8*^{+/+} endothelial cells derived from LLC, whereas the endothelial marker VE-cadherin (*VE-cad*) is present in both samples. *C*, an ~80 kDa TEM8 protein product is detectable only in *TEM8*^{+/+} tumor-derived endothelial cells (TECs) by immunoblotting. 293 cells stably transfected with TEM8 (293/TEM8) were used as a positive control. The band migrating at ~53 kDa is presumably nonspecific because it was detected by the secondary antibody alone. *D*, incisors are misaligned in the *TEM8*^{-/-} mice.

TEM8^{-/-} females to *TEM8*^{+/+} males. Both crossings produced a similar number of offspring, averaging 7.0 ± 1.4 (*TEM8*^{+/+} female) or 6.8 ± 0.5 (*TEM8*^{-/-} female) pups per litter (Supplementary Table S3). To confirm that the *TEM8* allele was deleted, we analyzed the expression of TEM8 mRNA and protein. For this, we isolated tumor endothelial cells from *TEM8* wild-type (WT) or KO mice because TEM8 is highly expressed in these cells (4). RT-PCR analysis of *TEM8* using PCR primer pairs downstream of the deleted exon 1 revealed *TEM8* mRNA expression in tumor endothelial cells isolated from *TEM8*^{+/+} but not *TEM8*^{-/-} mice (Fig. 1*B*, right). Similarly, Western blot analysis revealed TEM8 protein only in tumor endothelial cells of *TEM8* WT mice (Fig. 1*C*) when probed with an anti-TEM8 antibody (clone SB5), which bound to an epitope downstream of the deleted exon 1 (Supplementary Fig. S1). Taken together, these studies suggest that TEM8 protein is not expressed in our *TEM8*^{-/-} mice and that normal growth and development is, for the most part, unaffected by loss of TEM8.

A phenotype observed in adult *TEM8*^{-/-} mice, which became more pronounced with age, was a misalignment of their incisors (Fig. 1*D*). Continual growth of the incisors is normal in rodents but adult tooth size is usually controlled by interactive wear between

aligned upper and lower teeth. To prevent the abnormal tooth growth from interfering with food intake, incisors of the *TEM8*^{-/-} mice were routinely clipped. Over the course of 10 weeks, body weights of male and female *TEM8*^{-/-} mice were similar to their sex-matched *TEM8*^{+/+} littermates (Supplementary Fig. S2). Thus, as long as teeth were clipped, mutant mice seemed to develop normally without any other obvious behavioral or gross anatomic abnormalities.

In a further effort to identify defects in *TEM8*^{-/-} mice, we performed a comprehensive histologic analysis of adult mice. This analysis revealed mild to moderate increased ECM in several organs, including the ovaries, uterus, and skin (Fig. 2). In female mice, loose proteinacious ECM deposits were found throughout the ovaries, although follicles seemed to develop normally. In the uterus, increased ECM was noted in the lamina propria of the endometrium and, to a lesser extent, in the musculature. The metaphyseal periosteum of the femurs was mildly thickened due to increased ECM, and there was minimal periosteal thickening of the vertebra. Severe thickening of the periodontal ligament due to increased ECM was evident around the incisors and, to a lesser extent, around the molars. The excessive ECM in

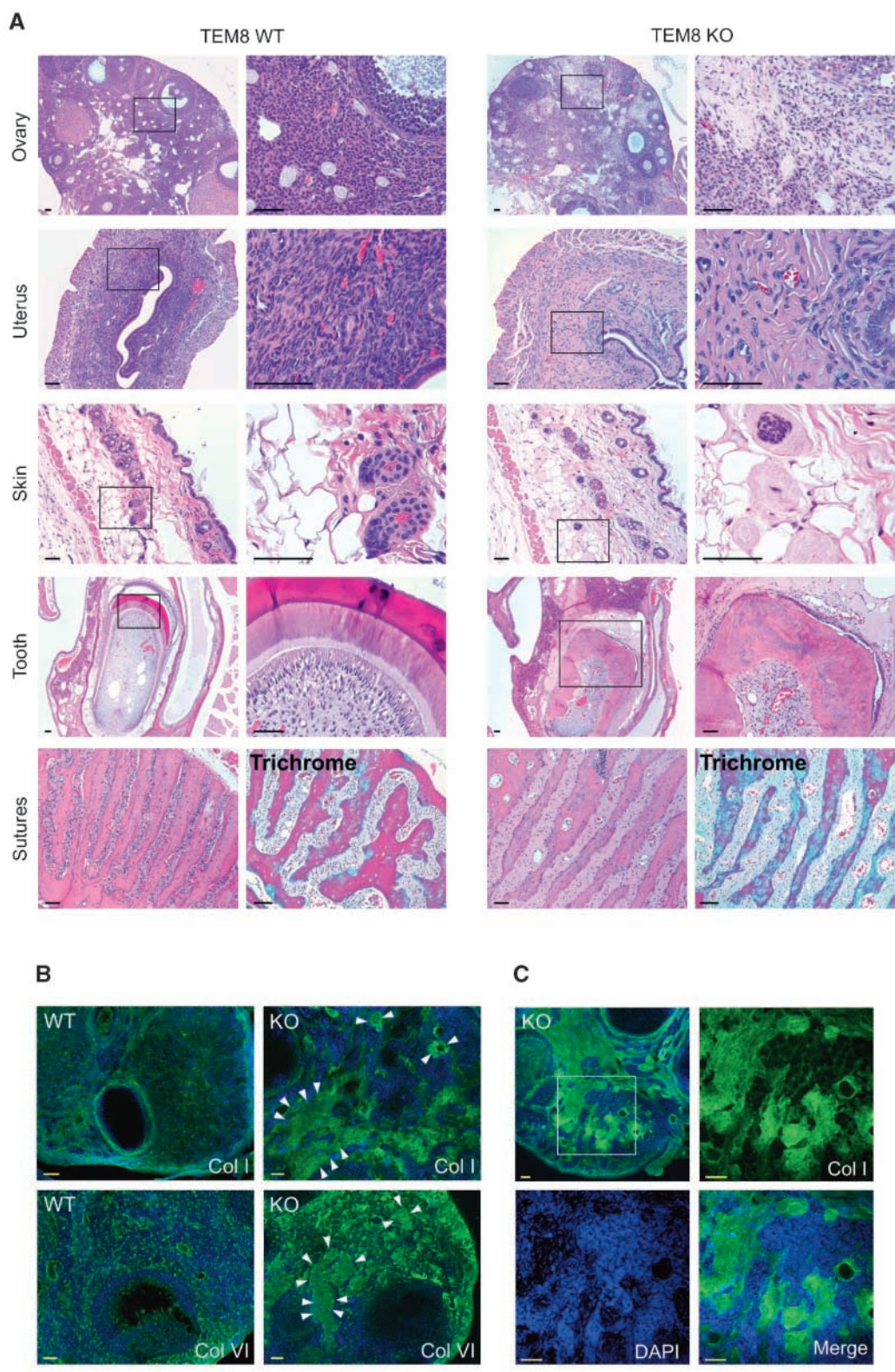


Figure 2. Histopathologic analysis. *A*, H&E staining of various organs. Note the increased ECM in each of the TEM8^{-/-} tissues. In the skin, the excess ECM surrounded the basal aspects of the hair follicles. Periodontal thickening was most severe at the incisors, with associated degeneration of ameloblasts and odontoblasts resulting in dental dysplasia. Trichrome staining revealed the collagen-like nature of the increased ECM (cranial sutures of the skull). *B*, immunofluorescence staining of the ovaries revealed focal up-regulation of collagen types I and VI (green) in the TEM8^{-/-} mice similar to the eosin staining in *A*. Arrowheads surround some of the more intensely stained pockets of collagen. *C*, the focal patches of collagen I (FITC, green) in the TEM8^{-/-} ovaries correspond to areas of low cell density [4',6-diamidino-2-phenylindole (DAPI), blue] when visualized under separate filters. Bar, 50 μm.

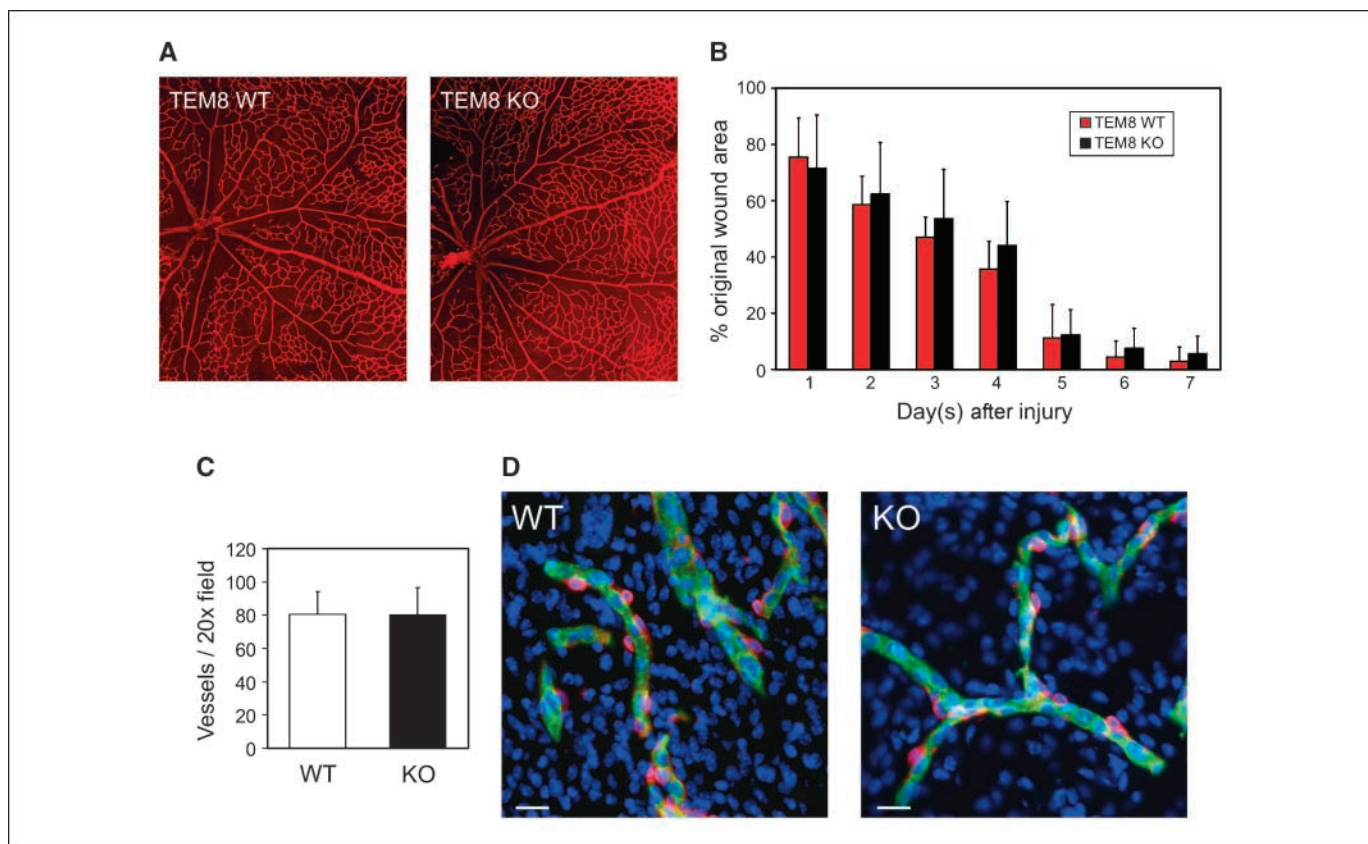


Figure 3. Physiologic angiogenesis is unaltered in $TEM8^{-/-}$ mice. Vessel structure at P10.5 in the developing retina (A), the rate of wound closure (B), the number of vessels in wounds (C), and vessel structure in the uterus (D) appeared similar between KO and WT mice. D, in the KOs, a decreased nuclear density (DAPI, blue) corresponding to areas with excessive ECM deposits (see Fig. 2) was frequently observed. Green, CD31-positive vessels; red, NG2-positive pericytes. Bar, 20 μ m.

the tissues surrounding the incisors presumably leads to their misalignment, which in turn results in a loss of normal abrasion and their eventual overgrowth. Associated degeneration of the enamel organ with resultant dental dysplasia was also consistent with the clinically noted incisor abnormalities. The cranial sutures of the skull were also thickened by increased ECM. More subtle increases in ECM were also noted in the lamina propria of the stomach, small and large intestines, urinary bladder, cervix, and tongue. Trichrome staining of the affected tissues suggested the excessive ECM to be collagen (Fig. 2A, bottom), but an increase in the number of fibroblasts was not evident. Because TEM8 has been found to bind collagen types I and VI *in vitro* (3, 6), we reasoned that disruption of TEM8 could potentially lead to a reduced uptake and degradation of these or other ECM proteins. Interestingly, immunofluorescence staining revealed focal deposits of collagen types I and VI in the $TEM8^{-/-}$ ovaries and uterus (Fig. 2B; Supplementary Fig. S3A), but other ECM proteins, such as laminin and fibrinogen, showed similar patterns of staining between KO and WT mice (data not shown). Western blotting also revealed increased levels of both collagen type I and collagen type VI protein in $TEM8$ -deficient tissues (Supplementary Fig. S3B).

We also analyzed $TEM8^{-/-}$ mice for defects in angiogenesis. First, the vessels of the developing retina, which form postnatally in rodents, were analyzed. From P0.5 to P10.5, no differences in vessel development or branching was noted in either the inner primary or outer vascular plexuses (Fig. 3A; data not shown). We also analyzed wound healing in adult mice but found no differences in the rate of

wound closure in $TEM8^{+/+}$ or $TEM8^{-/-}$ mice (Fig. 3B). Consistent with this result, immunofluorescence staining of vessels in wound sections failed to reveal differences in vessel numbers (Fig. 3C). We also compared angiogenesis using the mouse aortic ring assay and evaluated vascular endothelial growth factor-stimulated and fibroblast growth factor-stimulated angiogenesis using the directed *in vivo* angiogenesis assay (15), but again, no difference was found (data not shown). Vessel structures also seemed unaltered in the uterus (Fig. 3D) and ovaries, two of the tissues that displayed excess deposits of ECM.

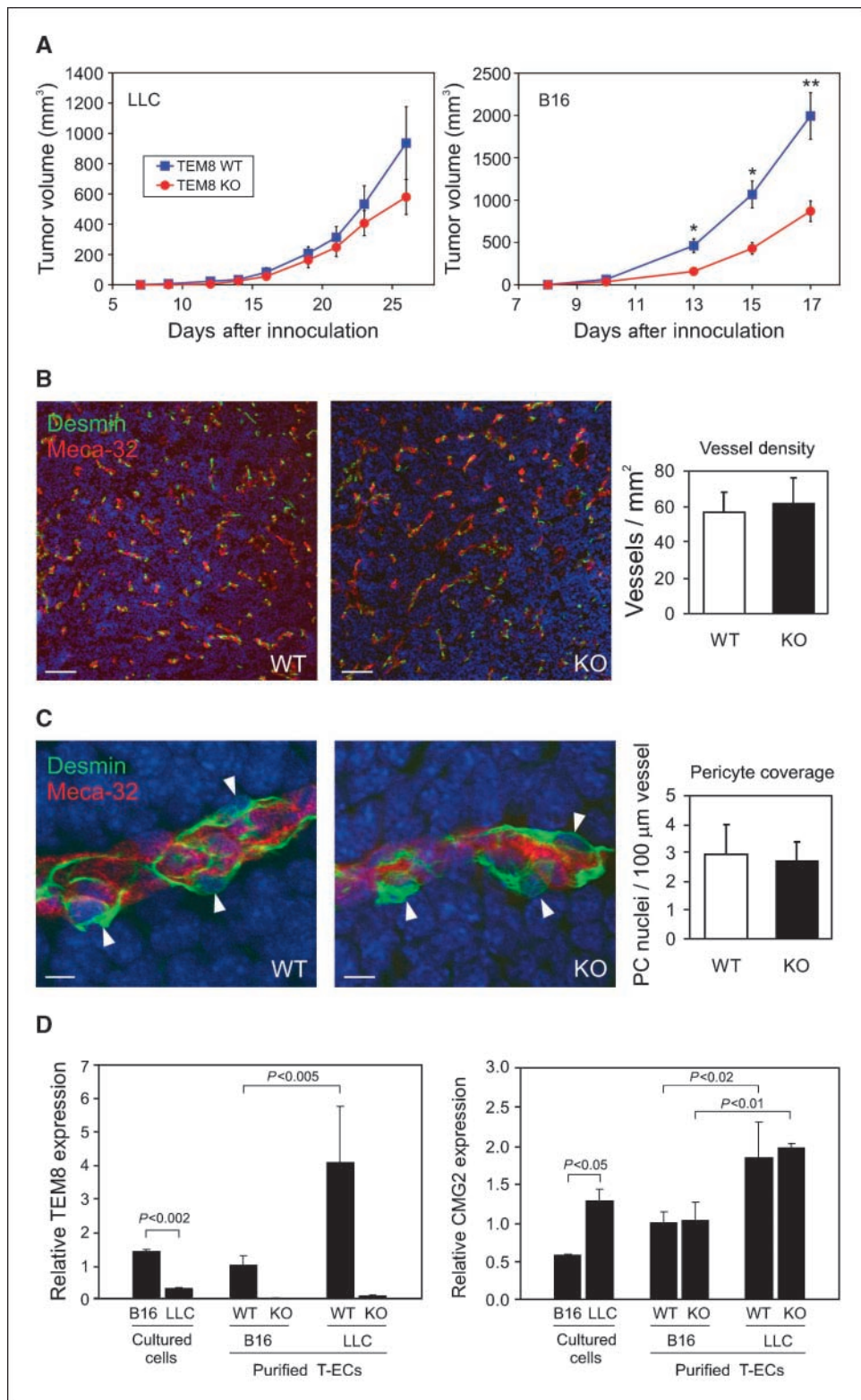
Because TEM8 is overexpressed in tumor vessels, we reasoned that it might be important for pathologic angiogenesis. To test this idea, $TEM8^{-/-}$ or $TEM8^{+/+}$ littermates were challenged s.c. with syngeneic Lewis lung carcinoma (LLC) or B16 melanoma tumors (Fig. 4A). Interestingly, B16 tumors grew slower in $TEM8^{-/-}$ compared with $TEM8^{+/+}$ mice, a result that was confirmed in four independent experiments. Although there seemed to be a slight delay in the growth of LLC tumors, the difference was not statistically significant. Thus, TEM8 expression in the host seems to preferentially promote the growth of certain tumor types.

To gain insight into possible mechanisms regulating the reduced B16 tumor growth in TEM8 mutant mice, we performed immunofluorescent staining of B16 tumor sections. An analysis of vessels using the endothelial marker PV-1 (Meca-32) did not reveal any differences in vessel density between $TEM8^{-/-}$ or $TEM8^{+/+}$ mice (Fig. 4B). Pericyte numbers were also unaltered (Fig. 4C). We also evaluated the number of proliferating endothelial

cells, the extent of hypoxia, and the level of apoptosis in tumors but again did not identify any differences between WT and KO mice (Supplementary Fig. S4). The number of host-derived inflammatory cells, such as CD68-positive macrophages, CD19-positive B cells, CD11b-positive myeloid cells, and CD18- or CD45-positive leukocytes, was also unchanged (data not shown).

Because B16 tumor growth seemed to depend more on host-derived TEM8 than LLC tumors, we expected that TEM8 might be expressed at a higher level in B16 tumor endothelial cells. To address this possibility, we performed qPCR on endothelial cells isolated from LLC or B16 tumors. The endothelial markers CD31 and VE-cadherin were highly enriched in the isolated endothelial cells

Figure 4. Evaluation of LLC and B16 tumors in TEM8^{+/+} and TEM8^{-/-} mice. **A**, tumor growth following s.c. tumor cell injection (*n* = 6–9 for LLC; *n* = 12–13 for B16). *Points*, mean; *bars*, SE. *, *P* < 0.005; **, *P* < 0.002 (Student's *t* test). **B**, vessel density in B16 tumors. Immunofluorescence staining of endothelial cells (Meca-32, red) and pericytes (desmin, green). *Bar*, 100 μm. **C**, number of pericytes in B16 tumors. *Arrowheads*, pericyte nuclei. *Bar*, 10 μm. **D**, qPCR analysis of TEM8 and CMG2 expression in B16 or LLC tumor cells in culture or purified tumor endothelial cells (T-ECs). *Columns*, mean biological replicates (separate flasks of cultured cells or independently isolated tumor endothelial cell samples); *bars*, SD.



Downloaded from <http://aacrjournals.org/cancerres/article-pdf/69/15/6025/12867152/6021.pdf> by guest on 03 February 2023

compared with unfractionated tumors (202- and 283-fold, respectively), confirming their purity (Supplementary Fig. S5). Unexpectedly, TEM8 mRNA levels were ~4-fold higher in LLC compared with B16 tumor endothelial cells, suggesting that reduced TEM8 expression in LLC tumor endothelial cells was not responsible for the noted differential effects on tumor growth (Fig. 4D). CMG2, on the other hand, was ~2-fold higher in cultured LLC tumor cells compared with B16 tumor cells and was ~2-fold higher in LLC versus B16 tumor-derived endothelial cells. Thus, CMG2 may share functional redundancy with TEM8, potentially contributing to the subdued response to TEM8 loss noted in the LLC tumor model. A possible redundant or overlapping function is supported by the fact that both TEM8 and CMG2 are able to bind anthrax toxin proteins (7, 8), both bind ECM molecules *in vitro* (3, 5, 6, 16), and deletion or mutation of either of these genes leads to excessive ECM (17, 18).

An important question is whether loss of TEM8 expression solely in endothelial cells is responsible for the B16 tumor growth delay and the excess ECM observed in certain organs or if pericytes, tumor-associated fibroblasts, or other host cell types are also involved. Our conditional KO mouse should provide a valuable tool for answering this question. TEM8^{-/-} mice will also provide a valuable tool for evaluating the role of TEM8 in anthrax-mediated toxicity *in vivo*.

Interestingly, mutations in the TEM8 homologue CMG2 have been found to cause the disorders juvenile hyaline fibromatosis and

infantile systemic hyalinosis (17, 18). These diseases are associated with the accumulation of amorphous uncharacterized ECM. In cell culture, CMG2 has been found to bind laminin and collagen type IV, whereas TEM8 has been found to bind collagen types I and VI (3, 6, 16). *In vivo*, we found focal overexpression of collagen types I and VI in TEM8^{-/-} mice. Taken together, these results suggest that both TEM8 and CMG2 play important roles in ECM homeostasis. That TEM8 promotes the growth of certain tumors suggests that antagonism of TEM8 function may be a useful strategy for the development of new anticancer agents.

Disclosure of Potential Conflicts of Interest

B. St. Croix: coinventor on a patent at Johns Hopkins University describing the use of TEMs as potential targets for cancer therapy. The other authors disclosed no potential conflicts of interest.

Acknowledgments

Received 3/25/09; revised 5/26/09; accepted 6/14/09; published OnlineFirst 7/21/09.

Grant support: Intramural Research Program of the National Cancer Institute, NIH, Department of Health and Human Services and federal funds from the National Cancer Institute under Contract No. HHSN26120080001E.

The costs of publication of this article were defrayed in part by the payment of page charges. This article must therefore be hereby marked *advertisement* in accordance with 18 U.S.C. Section 1734 solely to indicate this fact.

We thank Dr. Jill Dunty for purifying SB5 antibodies, members of the Mouse Cancer Genetics Program for helpful discussion, and Drs. Stephan H. Leppla and Shihui Liu for sharing unpublished data before publication.

References

- Kerbel RS. Tumor angiogenesis. *N Engl J Med* 2008;358:2039-49.
- St Croix B, Rago C, Velculescu V, et al. Genes expressed in human tumor endothelium. *Science* 2000;289:1197-202.
- Nanda A, Carson-Walter EB, Seaman S, et al. TEM8 interacts with the cleaved C5 domain of collagen $\alpha 3(\text{VI})$. *Cancer Res* 2004;64:817-20.
- Carson-Walter EB, Watkins DN, Nanda A, Vogelstein B, Kinzler KW, St Croix B. Cell surface tumor endothelial markers are conserved in mice and humans. *Cancer Res* 2001;61:6649-55.
- Hotchkiss KA, Basile CM, Spring SC, Bonucci G, Lisanti MP, Terman BI. TEM8 expression stimulates endothelial cell adhesion and migration by regulating cell-matrix interactions on collagen. *Exp Cell Res* 2005;305:133-44.
- Werner E, Kowalczyk AP, Faundez V. Anthrax toxin receptor 1/tumor endothelium marker 8 mediates cell spreading by coupling extracellular ligands to the actin cytoskeleton. *J Biol Chem* 2006;281:23227-36.
- Bradley KA, Mogridge J, Mourez M, Collier RJ, Young JA. Identification of the cellular receptor for anthrax toxin. *Nature* 2001;414:225-9.
- Scobie HM, Rainey GJ, Bradley KA, Young JA. Human capillary morphogenesis protein 2 functions as an anthrax toxin receptor. *Proc Natl Acad Sci U S A* 2003;100:5170-4.
- Abi-Habib RJ, Singh R, Leppla SH, et al. Systemic anthrax lethal toxin therapy produces regressions of subcutaneous human melanoma tumors in athymic nude mice. *Clin Cancer Res* 2006;12:7437-43.
- Rouleau C, Menon K, Boutin P, et al. The systemic administration of lethal toxin achieves a growth delay of human melanoma and neuroblastoma xenografts: assessment of receptor contribution. *Int J Oncol* 2008;32:739-48.
- Duesbery NS, Resau J, Webb CP, et al. Suppression of ras-mediated transformation and inhibition of tumor growth and angiogenesis by anthrax lethal factor, a proteolytic inhibitor of multiple MEK pathways. *Proc Natl Acad Sci U S A* 2001;98:4089-94.
- Liu S, Aaronson H, Mitola DJ, Leppla SH, Bugge TH. Potent antitumor activity of a urokinase-activated engineered anthrax toxin. *Proc Natl Acad Sci U S A* 2003;100:657-62.
- Liu S, Wang H, Currie BM, et al. Matrix metalloproteinase-activated anthrax lethal toxin demonstrates high potency in targeting tumor vasculature. *J Biol Chem* 2008;283:529-40.
- Seaman S, Stevens J, Yang MY, Logsdon D, Graft-Cherry C, St Croix B. Genes that distinguish physiological and pathological angiogenesis. *Cancer Cell* 2007;11:539-54.
- Guedez L, Rivera AM, Salloum R, et al. Quantitative assessment of angiogenic responses by the directed *in vivo* angiogenesis assay. *Am J Pathol* 2003;162:1431-9.
- Bell SE, Mavila A, Salazar R, et al. Differential gene expression during capillary morphogenesis in 3D collagen matrices: regulated expression of genes involved in basement membrane matrix assembly, cell cycle progression, cellular differentiation and G-protein signaling. *J Cell Sci* 2001;114:2755-73.
- Hanks S, Adams S, Douglas J, et al. Mutations in the gene encoding capillary morphogenesis protein 2 cause juvenile hyaline fibromatosis and infantile systemic hyalinosis. *Am J Hum Genet* 2003;73:791-800.
- Dowling O, Difeo A, Ramirez MC, et al. Mutations in capillary morphogenesis gene-2 result in the allelic disorders juvenile hyaline fibromatosis and infantile systemic hyalinosis. *Am J Hum Genet* 2003;73:957-66.